^{13}C NMR Study of Segmental Dynamics of Atactic Polypropylene Melts

N. E. Moe, XiaoHua Qiu, and M. D. Ediger*

Department of Chemistry, University of Wisconsin—Madison, Madison, Wisconsin 53706

Received November 2, 1999; Revised Manuscript Received January 13, 2000

ABSTRACT: ^{13}C NMR T_1 and NOE were measured for atactic polypropylene over the temperature range 325−425 K at ^{13}C Larmor frequencies of 25, 75, and 125 MHz. Because of the wide range of Larmor frequencies employed, the data discriminate among commonly used models for segmental dynamics; the modified KWW distribution function provides a much better fit than the DLM and the modified log χ^2 models. The temperature dependence of the segmental dynamics is very similar to that of the viscosity. An extrapolation of the calculated correlation times is consistent with previous NMR measurements near T_g. Interestingly, the full width half-maximum (fwhm) of the distribution of relaxation times remains unchanged at 1.3 decades, while previous NMR measurements nearer T_g reported a fwhm of 3.0 decades. Recent MD simulations are in qualitative agreement with the results reported here.

I. Introduction

The most important material property of an amorphous material, its glass transition temperature, is governed by the time scale of molecular motion.[1] At high temperatures, molecules can quickly rearrange, so any external stress applied to the material is easily relieved by deformation. As temperature is lowered to near T_g, this kind of motion becomes much slower, due to increased density and lower energy. The same material becomes resistant to deformation, reflected in a massive increase in the shear modulus and viscosity. The molecular motions whose slowing down cause the glass transition are thus of critical importance in understanding the relationship between chemical structure and T_g. T_g for polymers becomes independent of molecular weight at high molecular weights, implying that the large length scale relaxations of long polymers are irrelevant for this property. NMR experiments by Spiess and co-workers on polystyrene and atactic polypropylene using a number of different techniques showed that motion on the scale of a few repeat units approximately follows the temperature dependence of the viscosity from the high-temperature melt through the glass transition.[2,3] These results argue that very local rearrangements are the fundamental motions responsible for polymer flow.

One-dimensional ^{13}C NMR techniques have been used for more than 20 years to study polymer dynamics in the melt state.[4−6] The experimental observables T_1 and NOE depend on the reorientation of C−H bond vectors and thus probe dynamics most effectively on the length scale of a single repeat unit. Measured at a particular Larmor frequency ω, these observables are most sensitive to the dynamics that occur within a narrow frequency window. In principle, T_1 and NOE can be collected over a wide range of Larmor frequencies and temperatures to provide a detailed picture of the whole dynamic spectrum. In practice, a range of less than a factor of 5 in Larmor frequencies is typically used due to the limited availability of appropriate spectrometers. As a result, analysis of the NMR data often leads to ambiguous conclusions; i.e., usually more than one motional model can describe the experimental results.

We report here the first results of a project whose objective is to study the local dynamics of atactic polypropylene (aPP) over the widest possible range of frequencies and temperatures. We have completed T_1 and NOE measurements at 25.1, 75.4, and 125.7 MHz and temperatures from 315 to 420 K (extended to 525 K at 75.4 MHz). We chose to study aPP for a number of reasons. First, aPP is structurally the simplest polymer that does not crystallize and thus may be regarded as a model system for structurally more complex melts. Second, aPP has been a popular target for computer simulations,[7−10] and good dynamics data are required to evaluate the quality of these simulations. Previous experimental work on this polymer at high temperatures is unsatisfactory for this comparison as model-dependent parameters are given in place of T_1's.[6] Finally, Schaefer et al. have made measurements of the dynamics near T_g using 2D NMR techniques,[3] allowing comparison between the melt dynamics and the near-glassy dynamics.

Here we evaluate the ability of different motional models to describe the experimental T_1's and NOEs for aPP. We find a reasonable superposition of the experimental data at different Larmor frequencies using a temperature dependence similar to that of the viscosity. We test three bimodal relaxation time distributions, the DLM,[4] modified log χ^2,[11] and modified KWW (mKWW) functions, in global fits to the experimental data. The data decisively discriminate against the first two in favor of the mKWW. Fixing the temperature dependence of the relaxation times to that of the viscosity, the mKWW gives a much better fit than the DLM or the modified log χ^2. When the temperature dependence is treated as a free parameter, the DLM and the modified log χ^2 predict unphysical temperature dependencies. Finally, we compare our results to recent computer simulations of atactic polypropylene by Antonidas et al.[7]

II. Experimental Section

Materials. The atactic polypropylene sample was graciously provided by Dr. Lewis Fetters. Its microstructure has entirely head-to-tail linkages with absolutely random stereochemistry

* To whom all correspondence should be addressed.

10.1021/ma991844+ CCC: $19.00
Published on Web 03/01/2000

(M_w = 31 000 g/mol, M_w/M_n = 1.04). Details of the synthesis and characterization may be found in refs 12 and 13. Briefly, anionic polymerization of (*E*)-2-methyl-1,3-pentadiene leads to poly(1,3-dimethyl-1-butenylene). Hydrogenation of this polymer yields stereorandom polypropylene. This material is completely amorphous, in contrast to some products of commercial polymerization procedures which can be semicrystalline due to sequences of stereoregular repeat units. T_g was measured with DSC to be 270 K using 10 K/min heating/cooling rates and the midpoint convention.

Two different samples were prepared. For the first sample, used at 125.7 and 25.1 MHz, the bulk polymer was carefully degassed and sealed under N_2. This sample was placed in a 10 mm tube while a coaxial 5 mm tube containing perdeuterated dimethyl sulfoxide was inserted for locking purposes. The second sample, used at 75.4 MHz, was similarly degassed and placed in a 10 mm tube which was sealed under N_2 at a length of about 3 cm as required by the horizontal geometry of the homemade probe.

NMR Measurements. Three well-separated peaks were observed in the decoupled ^{13}C spectra at 21, 29, and 47 ppm, corresponding to the methyl, methyne, and methylene carbons, respectively. T_1 and NOE were measured at ^{13}C Larmor frequencies of 25.1, 75.4, and 125.7 MHz, using Bruker AC-100, DMX-300, and AM-500 spectrometers. Bruker high-resolution liquid-state probes were used at 25.1 and 125.7 MHz, while a homemade probe capable of sustaining higher temperatures was used at 75.4 MHz.

Protons were decoupled while collecting the T_1 spectra. T_1 was obtained by using a $\pi-\tau-\pi/2$ pulse sequence, waiting at least 5 times the methyl T_1 between each scan. Twelve or 16 delay times were used to determine the magnetization recovery curves, which were well described by single exponentials. NOE was measured by the comparison of spectra with continuous decoupling and inverse-gated decoupling. The number of scans used for signal averaging ranged from 8 at 125.7 MHz to 48 at 25.1 MHz, while more scans were collected at each frequency at the lowest temperatures to compensate for the broader lines.

On the AC-100 and AM-500 spectrometers, temperature was measured before and after each experiment by inserting into the probe a tube containing a platinum resistance thermometer in DMSO. The average of the two temperatures was taken to be the experimental temperature; the two temperatures usually agreed within 1 K. The reported numbers are believed to be accurate to within 1 K. On the DMX-300 instrument, the temperature was calibrated using six samples of known melting points. The calibration curves taken before and after the set of experiments were accurate to within 1 K while the fluctuations during a given experiment were ≤0.1 K.

Relaxation Equations. The only important mechanism leading to magnetization relaxation in this system is dipole−dipole interaction between ^{13}C nuclei and directly bound protons. Relaxation occurring by CSA was determined to be negligible, and spin rotation is excluded because the NOEs at the highest temperatures reach a high plateau value. For the case of dipole−dipole relaxation, the equations which relate the observed T_1 and NOE with the dynamics of C−H bond vectors are as follows:

$$\frac{1}{T_1} = Kn[J(\omega_H - \omega_C) + 3J(\omega_C) + 6J(\omega_H + \omega_C)] \quad (1)$$

$$\mathrm{NOE} = 1 + \frac{\gamma_H}{\gamma_C}\left[\frac{6J(\omega_H + \omega_C) - J(\omega_H - \omega_C)}{J(\omega_H - \omega_C) + 3J(\omega_C) + 6J(\omega_H + \omega_C)}\right] \quad (2)$$

where ω_H and ω_C are the resonance frequencies of hydrogen and carbon; $\omega_H = 3.977\omega_C$. K is a constant and is taken to be 2.29×10^9 s^{-2} following ref 14, n is the number of bonded protons, and γ_H and γ_C are the gyromagnetic ratios for hydrogen and carbon. $J(\omega)$ is the spectral density function and

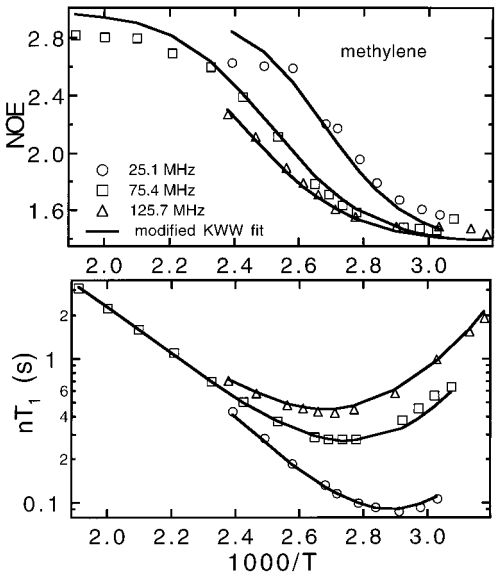

Figure 1. ^{13}C NMR T_1 and NOE results as a function of temperature and Larmor frequency for the methylene carbon in atactic polypropylene. The solid lines are the best fit using the modified KWW distribution function.

is the Fourier transform of the second-order autocorrelation function $G(t)$

$$J(\omega) = \frac{1}{2}\int_{-\infty}^{+\infty} G(t)e^{i\omega t}\,dt \quad (3)$$

$$G(t) = \langle 3\cos^2\Theta(t) - 1\rangle/2 \quad (4)$$

where $\Theta(t)$ describes the orientation of a C−H bond vector at time t relative to its orientation at time $t = 0$. The area under $G(t)$ defines the correlation time τ_c

$$\tau_c = \int_0^\infty G(t)\,dt \quad (5)$$

Large τ_c's imply a slowly decaying $G(t)$ and slow dynamics.

An equivalent way to represent C−H vector dynamics is to consider a distribution of motional time constants $F(\tau)$ which contribute to the relaxation. $F(\tau)$ is related to $G(t)$ by the Laplace transform:

$$G(t) = \int_0^\infty F(\tau)e^{-t/\tau}\,d\tau \quad (6)$$

III. Results

Figures 1−3 present the experimental data plotted along with the best fit using a model function, as described later. Most of the points at 25.1 and 125.7 MHz represent averages of two or three individual experiments, while most of the points at 75.4 MHz represent single experiments. Reproducibility near the T_1 minima is better than 2% and is generally within 5% elsewhere, while NOE is known within 0.1. The precision of the measurements at 75.4 MHz is somewhat better. At low temperatures, broad lines tend to reduce precision. Reproducibility is also generally worse near the high-temperature limits of the Bruker probes. Tabulated data at all frequencies and temperatures can be found in the Supporting Information.

IV. Time−Temperature Superposition

A common procedure when analyzing the results of mechanical experiments is to construct master curves from measurements of the modulus at different tem-

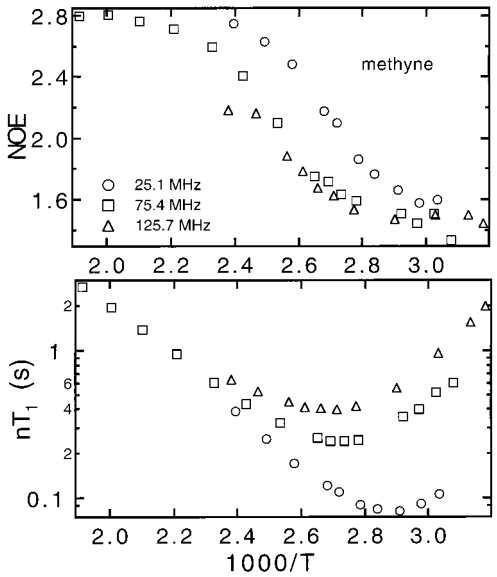

Figure 2. ^{13}C NMR T_1 and NOE results for the methyne carbon as a function of temperature and Larmor frequency.

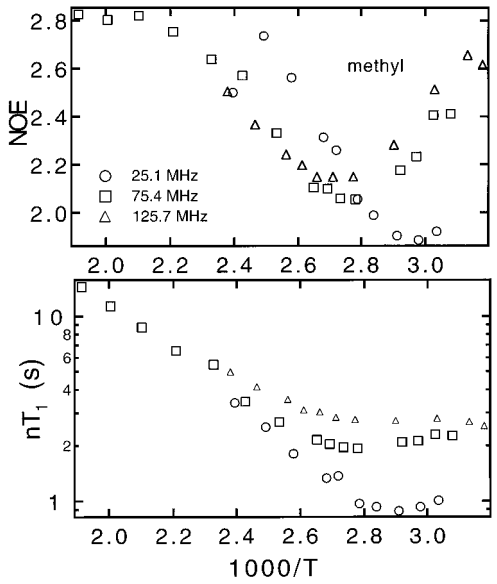

Figure 3. ^{13}C NMR T_1 and NOE results for the methyl carbon as a function of temperature and Larmor frequency.

peratures.[1] This procedure works exactly when all the components of the relaxation time distribution have the same temperature dependence. Analogously, superposition of T_1's and NOEs taken at different Larmor frequencies works when all the molecular processes that influence these observables have the same temperature dependence. Time−temperature superposition has been approximately fulfilled for NMR observables in many polymer systems.[14−17] The task of finding a motional model to describe the NMR data is greatly simplified if the shape of $F(\tau)$ can be considered temperature independent. Here we follow the example of Guillermo et al.[15] and plot $\log(nT_1(T)/\omega_c)$ versus $\log(\omega_c\tau_c(T))$, where $\tau_c(T)$ is the temperature dependence of the correlation times. Similarly, we also plot NOE versus $\log(\omega_c\tau_c(T))$. The results shown in Figure 4 confirm that, for aPP over this range of temperatures and frequencies, the shape of $F(\tau)$ is approximately constant.

The temperature dependence which provides the superposition in Figure 4 is described by the VTF

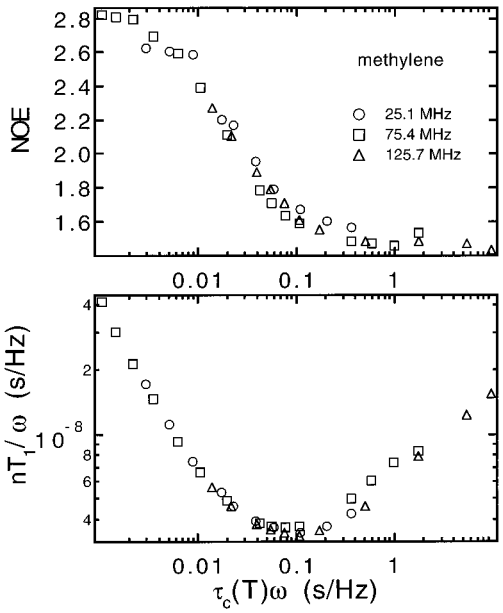

Figure 4. Time−temperature superposition plot for T_1 and NOE at different Larmor frequencies. The reasonable success of this superposition implies that the shape of the distribution of relaxation times is temperature independent.

equation (equivalent to the WLF equation)

$$\log\left(\frac{\tau}{\tau_\infty}\right) = \frac{B}{T - T_0} \tag{7}$$

For convenience, we chose the constants B and T_0 to be 560 and 214 K, respectively, in accordance with the global fit results using the modified KWW (mKWW) function (see below). These are quite similar to the values of 586 and 224 K reported for the temperature dependence of the viscosity.[13] However, the test for time−temperature superposition is not dependent on the validity of any particular model for the correlation function shape. The superposition procedure does not "know" if the temperature dependence comes from fitting the NMR data to any particular model for $F(\tau)$. Thus, without input from any model we could have achieved at least as successful a superposition.

V. Fits to Models

The experimental T_1's and NOEs are related to the dynamics of C−H bond vectors through eqs 1−4. In the extreme narrowing regime where T_1 is independent of Larmor frequency (i.e., $J(\omega)$ is a constant) these equations simplify; NOE is about 3, and T_1 is inversely proportional to τ_c. At lower temperatures, no simplification is possible, and it is generally impossible to extract physical parameters such as τ_c or an activation energy from the raw data without the help of a model. However, the experimental results in this region are sensitive to the *shape* of the correlation function and are able in principle to differentiate between good and bad models. All the data presented here lie outside of the extreme narrowing regime.

We fit our data using three different models for $J(\omega)$: the DLM,[4] modified log χ^2,[11] and mKWW. These models are bimodal distributions of relaxation times; each has a high-frequency Lorentzian component weighted by the value "a" and a lower frequency, broad distribution weighted by $(1 - a)$. Previous work has shown this form

to be more successful than unimodal distributions.[4,11,18] The functional forms of the three models follow:

For the DLM model

$$J_{\mathrm{DLM}}(\omega) = \frac{a\tau_0}{1 + (\omega\tau_0)^2} + \frac{1 - a}{(\alpha + i\beta)^{1/2}} \tag{8}$$

where $\alpha = \tau_2^{-2} + 2\tau_1^{-1}\tau_2^{-1} - \omega^2$ and $\beta = 2\omega(\tau_1^{-1} + \tau_2^{-1})$. The time constants are arranged $\tau_0 < \tau_1 < \tau_2$. The DLM distribution is derived from a microscopic model for the local dynamics and so has an attractive theoretical basis.[19] In the original model, τ_1 is associated with cooperative transition pairs and τ_2 with isolated conformational transitions. The range spanned by $(\tau_2^{-1} + 2\tau_1^{-1})^{-1}$ and τ_2 determines the width of the distribution of relaxation times.

For the modifed log χ^2 model

$$J_{\mathrm{mlog}\chi^2}(\omega) = \frac{a\tau_0}{1 + (\omega\tau_0)^2} + (1 - a)\int_0^\infty \frac{\tau_1 F^{(p)}(s)[b^s - 1]\,\mathrm{d}s}{(b - 1)[1 + (\omega\tau_1)^2((b^s - 1)/(b - 1))^2]} \tag{9}$$

where $F^{(p)}(s)\,\mathrm{d}s = (1/\Gamma(p))(ps)^{p-1}\mathrm{e}^{-ps}p\,\mathrm{d}s$ and $s = \log_b[1 + (b - 1)\tau/\tau_1]$. The logarithmic base b is set equal to 1000 by convention. The parameter p determines the width of the distribution (small p corresponds to a broad distribution). This empirical distribution is asymmetric, skewed toward longer times. The integral in eq 9 was evaluated numerically.

For the mKWW model

$$J_{\mathrm{mKWW}}(\omega) = \frac{a\tau_0}{1 + (\omega\tau_0)^2} + (1 - a)\sum_{i=1}^{n} F_{\mathrm{KWW}}(\tau_i)\left[\frac{\tau_i}{1 + (\omega\tau_i)^2}\right] \tag{10}$$

We used the series method of calculating $F_{\mathrm{KWW}}(\tau)$ given by Lindsey and Patterson[20]

$$F_{\mathrm{KWW}}(\tau_i) = -\frac{\tau_1}{\pi\tau_i}\sum_{k=0}^{\infty}\frac{(-1)^k}{k!}\sin(\pi\beta k)\Gamma(\beta k + 1)\left(\frac{\tau_i}{\tau_1}\right)^{\beta k+1} \tag{11}$$

where Γ is the gamma function and β is related to the width of the distribution; $\beta = 1.0$ recovers a single exponential, and $\beta < 1$ represents a broader distribution. Equation 11 was evaluated using REAL*16 double precision in FORTRAN 77 and over a range of τ_i, generating a distribution of single exponentials τ_i that approximate the continuous function. Here the sum of $F_{\mathrm{KWW}}(\tau_i)$ is normalized

$$\sum_{i=1}^{n} F_{\mathrm{KWW}}(\tau_i) = 1.0 \tag{12}$$

The time domain representation of the mKWW function is

$$G(t) = a\exp\left(\frac{-t}{\tau_0}\right) + (1 - a)\exp\left(-\left(\frac{t}{\tau_1}\right)^{\beta}\right) \tag{13}$$

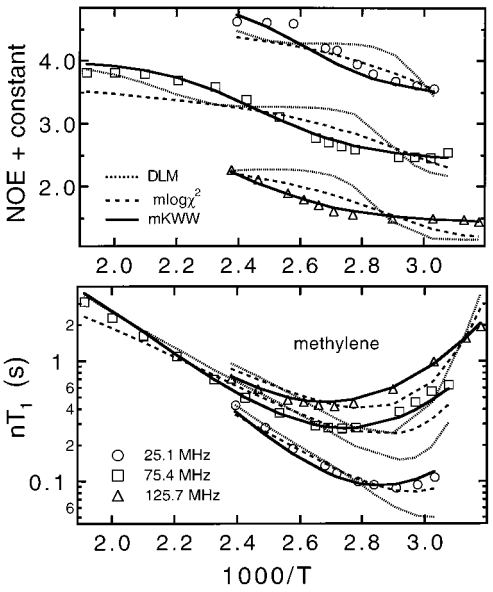

Figure 5. Results of global fits using the DLM, modified log χ^2, and modified KWW distribution functions; the temperature dependence is constrained to be that of the viscosity reported in ref 12. The NOEs at 25.1 MHz are offset by +2.0 and the NOEs at 75.4 MHz are offset by +1.0 for clarity. Only the modified KWW distribution can provide a reasonable description of the data.

The first term in eqs 8, 9, and 10 is a single Lorentzian whose time constant τ_0 needs to be short compared to the inverse of the Larmor frequency. Computer simulations have linked this fast component with librational motions,[21] which are unlikely to have a strong temperature dependence. Accordingly, we set $\tau_0 = 1$ ps independent of temperature.[22] τ_2/τ_1 for DLM, p for modified log χ^2, and β for mKWW were fixed to be temperature independent, as suggested by successful time−temperature superposition. We assumed a WLF temperature dependence for all time constants other than τ_0, first constraining the values of B and T_0 to match the viscosity and later allowing them to vary freely.

The best fits were obtained by simultaneously fitting all the methylene T_1 and NOE data at all three Larmor frequencies and all temperatures. A grid search method was used that evaluated many combinations of the model parameters. The fits obtained were determined to be very near to the absolute best fits by systematically narrowing the width of parameter space searched about the previously determined best fit. The best fits to the methylene T_1's and NOEs using the DLM, modified log χ^2, and mKWW models are shown in Figures 5 and 6. As mentioned previously, Pschorn et al. found that the temperature dependence of the local dynamics approximately matches that of the viscosity in polystyrene.[2] In anticipation that aPP would behave similarly, we first constrained B and T_0 from eq 7 to be 586 and 224 K, respectively, following ref 13. These results are plotted in Figure 5. Figure 6 shows the results obtained when the temperature dependence was allowed to vary freely. The fitting parameters are collected in Tables 1 and 2.

Discussion of Fit Results. Figure 5 shows that the mKWW function provides a much better description of the experimental results than either the DLM or the modified log χ^2 distributions. In Figure 6, where the temperature dependence is no longer constrained to that of the viscosity, these other two models do provide much

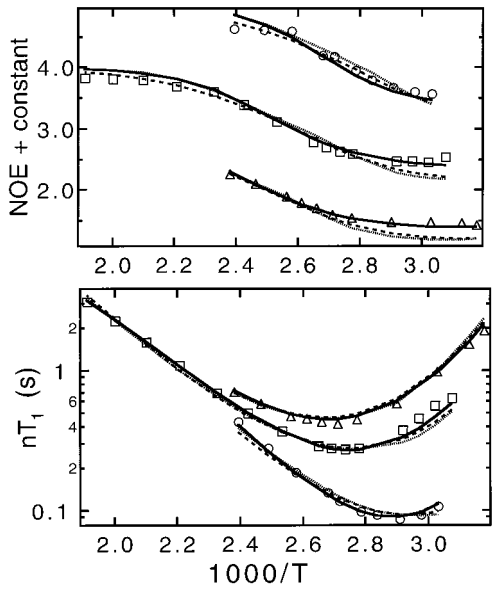

Figure 6. Results of global fits using the DLM, modified log χ^2, and modified KWW distribution functions; the temperature dependence is allowed to vary freely. The symbols are the same as in Figure 5. Again, the modified KWW function provides the best fit.

Table 1. Best Fit Parameters to Methylene and Methyne Data Fixing the Temperature Dependence To Be That of the Viscosity (T_0 = 224 K and B = 586 K)

carbon	model	τ_0 (ps)[a]	τ_1 (ps)[b]	τ_2 (ps)[b]	a	p	β
methylene	DLM	1.0	170	32000	0.00		
methylene	modified log χ^2	1.0	440		0.21	11	
methylene	modified KWW	1.0	720		0.27		0.43
methyne	modified KWW	1.0	840		0.22		0.44

[a] Constrained at this value independent of temperature. [b] Value at 369 K.

improved fits. However, two observations can be made. First, the mKWW function still provides a qualitatively better fit, and second, the optimal temperature dependence derived from the DLM and modified log χ^2 models is completely different from the temperature dependence of the viscosity. As discussed in the next section, the predicted temperature dependence for these two models over the experimental range is nearly Arrhenius and leads to no hope of reconciliation with 2D NMR results[3] near T_g. Figure 7 shows the distribution of relaxation times $F(\tau)$ for all three distributions for the fits that were constrained to follow the temperature dependence of the viscosity. The librational component is not displayed in this figure.

This discrimination among different popular models is largely due to the wide temperature and frequency range available for this study. As a test, we also ran a global fit using the modified log χ^2 function on a reduced data set which discarded the two or three lowest temperature points at each frequency (not shown). The result was an acceptable fit, equivalent to the mKWW fit.

The mKWW fits the data well over the entire frequency and temperature range excepting only the highest temperature NOEs taken at 75.4 MHz; the fit values approach 3 (the extreme narrowing regime) too rapidly. At high temperature, the long time components of $F(\tau)$ are brought into the frequency window of the NMR experiments, and our results indicate that some relaxation occurs at lower frequencies than are represented by the mKWW distribution. This deficiency could be remedied by adding another, very long-time component to the mKWW distribution, the existence of which has experimental and theoretical justification.[23] More data at lower Larmor frequencies will help to clarify this part of the distribution.

We also found that the mKWW provided a good fit to the methyne carbon data using a similar temperature dependence as used for the methylene carbon. Fit parameters are listed in Tables 1 and 2. As the values of nT_1 and NOE are similar for methylene and methyne carbons, the relaxation time distributions describing their dynamics are also quite similar.

No fit was attempted for the methyl data, since methyl rotation is a dominant feature and not directly connected to segmental dynamics. None of the models described here are appropriate without modification. The methyl data also have some puzzling features such as a minimum in NOE that may make it difficult to fit the data.

VI. Comparison with Other Results on Atactic Polypropylene

NMR. Atactic polypropylene has previously been studied in the melt and near-glassy states using NMR. Dekmezian et al. used ^{13}C NMR to study the dynamics of the melt, but do not report experimental T_1's or NOEs and include only an average correlation time extracted using the log χ^2 model.[6] Schaefer et al. used solid-state 2D exchange experiments to measure correlation times in the vicinity of T_g.[3] Some complications arise because the various samples used in these two studies and our own have different T_g's. The differences in T_g are due to the different microstructures and molecular weights of the various samples. To facilitate comparison of results on the different samples, the temperature axis of Figures 8 and 9 is scaled $1000/(T + (270\text{ K} - T_g))$, where 270 K is the T_g of our sample.

Figure 8 brings together the high-temperature experimental correlation times given by Dekmezian et al. using the log χ^2 model (without the additional single Lorenzian in eq 9) with those derived from the best fit to our data using the mKWW function. These values are in closer agreement with our data after the difference in T_g's of the two samples is accounted for. Given the inability of even the modified log χ^2 model to describe our results over the full frequency and temperature range, the remaining discrepancies are likely attributable to the inadequacies of the log χ^2 model.

Figure 9 compares the temperature dependence extracted from our results at high temperature with correlation times for C−H vector reorientation reported by Schaefer et al.[3] near T_g. The extrapolation of the best fit results using the mKWW function (solid line) does not have a strong enough temperature dependence to intersect the solid-state NMR results. However, since the T_g reported for Schaefer's sample is 17 K lower than sample used in this study, it is not straightforward to compare the temperature dependence of the two. The fit using the mKWW and the temperature dependence of the viscosity (dashed−dotted line) may provide a better connection. Over our experimental temperature range, though, these two temperature dependencies are not very different, nor are the qualities of the fits in Figures 5 and 6. A comparison of the mKWW distribution results with the temperature dependencies coming

Table 2. Best Fit Parameters to Methylene and Methyne Data

carbon	model	τ_0 (ps)[a]	τ_1 (ps)[b]	τ_2 (ps)[b]	a	p	β	T_0 (K)	B (K)
methylene	DLM	1.0	960	4500	0.53			119	1120
methylene	modified log χ^2	1.0	1050		0.51	45		104	1340
methylene	modified KWW	1.0	800		0.39		0.54	214	560
methyne	modified KWW	1.0	840		0.35		0.55	219	520

[a] Constrained at this value independent of temperature. [b] Value at 369 K.

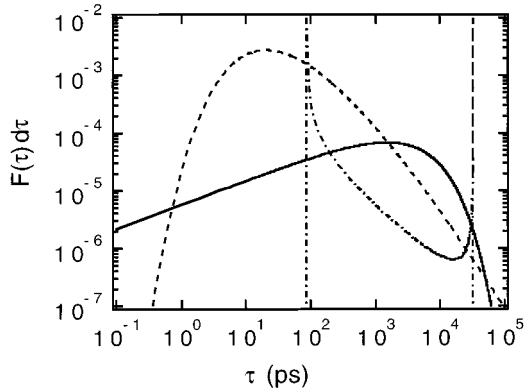

Figure 7. Three distribution functions considered in this paper: the DLM (– · –), modified log χ^2 (– – –), and modified KWW (—) plotted at 369 K. These curves are the best fit results obtained while fixing the temperature dependence to that of the viscosity.

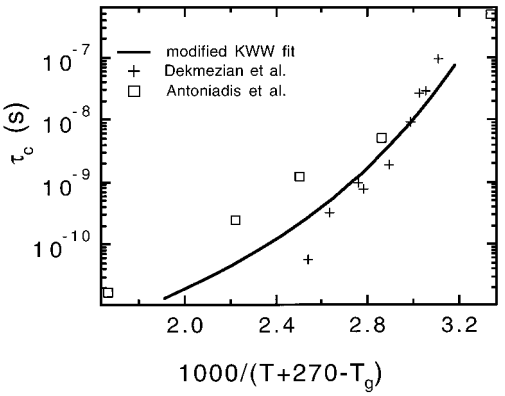

Figure 8. Correlation times from the modified KWW fit, from previous NMR experiments by Dekmezian et al.,[6] and from molecular dynamics simulations by Antoniadis et al.[7] The temperature for the results by Dekmezian et al. has been shifted by 17 deg relative to our results to account for the lower T_g of their sample.

from the DLM (dotted line) and modified log χ^2 functions (dashed line) shows that these two models offer no hope of reconciliation with the low-temperature results. These models predict nearly Arrhenius behavior.[24] Figure 10 shows a comparison of the distribution of relaxation times for segmental dynamics of aPP for this study and the one from solid-state NMR measurements[3] near T_g. It is interesting to notice that the distribution of relaxation time for this study remains unchanged at 1.3 decades full width half-maximum (fwhm) from $T_g + 45$ K to $T_g + 150$ K. On the other hand, the distribution reported by Schaefer from T_g to $T_g + 15$ K has a fwhm of 3 decades. This difference in the distribution of relaxation time partly explains why the extrapolation of our experimental results does not fully agree with the solid-state measurements as shown in Figure 9, since a temperature-independent distribution of relaxation times is assumed in the former case. The strong temperature dependence of the distribution of relaxation times as T_g is approached is consistent with the prediction of a model employing spatially heterogeneous dynamics near T_g.[25]

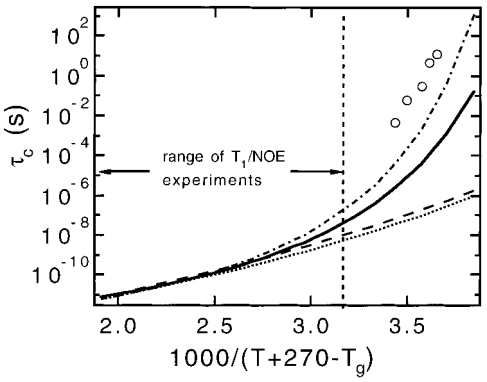

Figure 9. Correlation times from the best modified KWW fit (temperature dependence constrained to the viscosity's (– · –); free temperature dependence (—)), the DLM fit (· · ·), and the modified log χ^2 fit (– – –) (both free temperature dependence). The circles are from solid-state NMR experiments by Schaefer et al.,[3] which have been shifted by 17 deg relative to our results to account for the lower T_g of their sample. Only the modified KWW fits can be successfully extrapolated to lower temperatures.

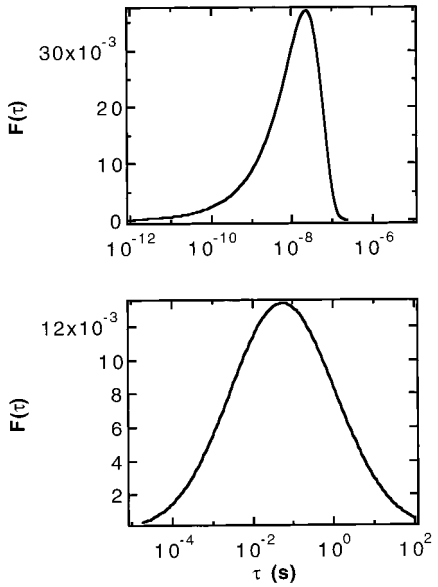

Figure 10. Distribution of relaxation times for the segmental dynamics for atactic polypropylene from this study is plotted in the top panel. The distribution shape remains unchanged for experimental temperatures from $T_g + 45$ K to $T_g + 150$ K. The lower panel shows the distribution of relaxation time found by Schaefer et al.[3] near T_g. The strong temperature dependence of distribution of relaxation times near T_g are consistent with a model employing spatially heterogeneous dynamics near T_g.

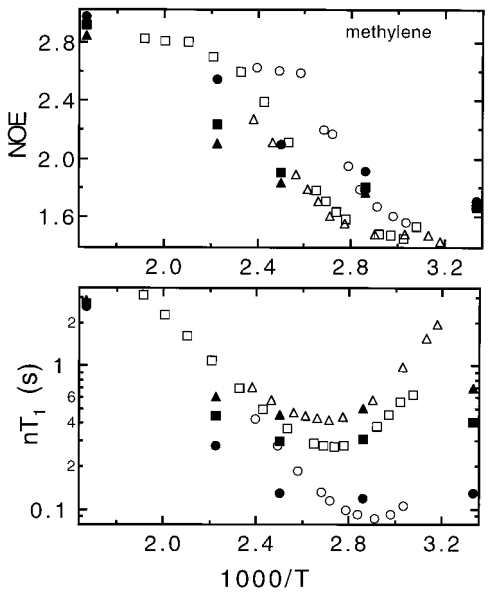

Figure 11. Comparison of experimental T_1's and NOEs with those calculated from molecular dynamics simulations by Antoniadis et al.[7] The open symbols correspond to the experimental results and the solid symbols to the simulations. The circles represent 25.1 MHz, the squares 75.4 MHz, and the triangles 125.7 MHz.

Molecular Dynamics Simulations. The NMR results in this work probe the local dynamics of aPP on the nanosecond time scale. They are thus able to provide an ideal check on molecular dynamics simulations. Conversely, simulations are in a good position to provide a molecular level interpretation of the NMR results.

We briefly compare our NMR results with recent simulations of aPP by Antoniadis et al.[7] The model system consisted of two molecules each with 76 repeat units, and the trajectories were 1 ns in length. Correlation functions for the methyl−methyne C−C bond vectors were reported, allowing comparison with NMR T_1 and NOE via eqs 1−4.[26] Figure 11 shows that the predictions of T_1 and NOE do not agree well with the experimental results; the shapes of the temperature-dependent curves are also qualitatively incorrect. The squares in Figure 8 show the correlation times calculated in ref 7. The simulated dynamics are within an order of magnitude of the best mKWW fit to the experiments but are too long.[27] We are optimistic that better agreement with experiments will come with further refinement of simulation parameters.

Rheology. In contrast to our findings in a study of polyethylene,[28] the temperature dependence of segmental dynamics of aPP is very close to the temperature dependence of the viscosity.[13] Thus, for aPP, it is reasonable to imagine that the large-scale rearrangement of chain conformation required for flow is simply the result of many independent conformational transitions. Studies on other polymers, such as polystyrene,[2] also found that local dynamics have a temperature dependence that is quite similar to that of the viscosity, suggesting that the conformational transitions are the fundamental motions for flow for most polymers. Because of its lack of side groups, polyethylene is a prominent exception.[28]

VII. Concluding Remarks

We have reported ^{13}C NMR T_1 and NOE results as a function of Larmor frequency and temperature for atactic polypropylene. Larmor frequencies ranged from 25 to 125 MHz, and temperatures varied from 315 to 525 K. We found that the data at different frequencies could be reasonably superimposed, in accordance with the principle of time−temperature superposition. We performed global fits of the experimental data using three different model distributions under conditions of a temperature-independent width for $F(\tau)$. The mKWW function provided a good fit while giving a WLF temperature dependence similar to that of the viscosity. The DLM and modified log χ^2 distributions failed to describe the data and predicted nearly Arrhenius temperature dependencies.

Relaxation time measurements have an important role to play in more complex polymer systems, such as polymer blends. In order for the potential of these measurements to be fully exploited, however, it must be possible to unambiguously deduce the segmental relaxation time distribution for each component as a function of temperature. The work presented here takes one important step toward that goal by showing that the segmental relaxation time distribution in a one-component system can be accurately characterized with measurements over a wide range of fields and temperatures.

We are currently collecting T_1 and NOE at lower Larmor frequency (5 MHz) and extending the temperature range of the 25.1 MHz measurements. We also plan to measure $T_{1\rho}$, which will provide information about very low-frequency components of $J(\omega)$. This new data will present a number of opportunities. First, a more stringent test can be made for the mKWW distribution, which after all is only an empirical function. Additional data at high temperature and low frequency will help to define any long-time tail in the correlation function lacking in the mKWW description. A wider frequency range at a particular temperature should also allow us to further test time−temperature superposition in atactic polypropylene. Finally, it remains to be seen how universally applicable the mKWW distribution, or one slightly more complex, is for describing the high-temperature local dynamics of amorphous polymers.

Acknowledgment. This research is supported by the National Science Foundation through the Division of Material Research, Polymer Program (DMR-9732483). Part of the study was performed on a variable field NMR instrument supported by NSF CHE 95-08244. Other parts of the study were performed in the Instrument Center of the Department of Chemistry, University of Wisconsin−Madison. Those instruments are supported by NSF CHE-8306121 and NIH 1 S10 RR02388-01. We thank Dr. Wei Zhu, Prof. Tom Farrar, Dr. Charlie Fry, Marvin Kontney, and Tom Ferris for their support.

Supporting Information Available: Tables of T_1 and NOE data at 25, 75, and 125 MHz. This material is available free of charge via the Internet at http://pubs.acs.org.

References and Notes

(1) See for example: Aklonis, J. J.; MacKnight, W. J. *Introduction to Polymer Viscoelasticity*; Wiley: New York, 1983.
(2) Pschorn, U.; Rossler, E.; Sillescu, H.; Kaufmann, S.; Schaefer, D.; Spiess, H. W. *Macromolecules* **1991**, *24*, 398.
(3) Schaefer, D.; Spiess, H. W.; Suter, U. W.; Fleming, W. W. *Macromolecules* **1990**, *23*, 3431.

(4) Dejean de la Batie, R.; Laupretre, F.; Monnerie, L. *Macromolecules* **1989**, *23*, 3431.
(5) Schaefer, J. *Macromolecules* **1973**, *6*, 882.
(6) Dekmezian, A.; Axelson, D.; Dechter, B.; Mandelkern, L. *J. Polym. Sci., Polym. Phys. Ed.* **1985**, *23*, 367.
(7) Antoniadis, S. J.; Samara, C. T.; Theodorou, D. N. *Macromolecules* **1998**, *31*, 7944.
(8) Kuhn, B.; Ehrig, M.; Ahlrichs, R. *Macromolecules* **1996**, *29*, 4051.
(9) Han, J.; Boyd, R. H. *Macromolecules* **1994**, *27*, 5365.
(10) Theodorou, D. N.; Suter, U. W. *Macromolecules* **1985**, *18*, 1467.
(11) Zhu, W.; Ediger, M. D. *Macromolecules* **1995**, *28*, 7549.
(12) Zhongde, X.; Mays, J.; Xuexin, C.; Hadjichristidis, N.; Schilling, F. C.; Bair, H. E.; Pearson, D. S.; Fetters, L. J. *Macromolecules* **1985**, *18*, 2560.
(13) Pearson, D. S.; Fetters, L. J.; Younghouse, L. B.; Mays, J. W. *Macromolecules* **1988**, *21*, 478.
(14) Gisser, D.; Glowinkowski, S.; Ediger, M. D. *Macromolecules* **1991**, *24*, 4270.
(15) Guillermo, A.; Dupeyre, R.; Cohen-Addad, J. P. *Macromolecules* **1990**, *23*, 1291.
(16) Tylianakis, E.; Dais, P.; Andre, I.; Taravel, F. F. *Macromolecules* **1995**, *28*, 7962.
(17) Ravindranathan, S.; Sathyanarayana, D. N. *Macromolecules* **1996**, *29*, 3525.
(18) Gisser, D. J.; Ediger, M. D. *Macromolecules* **1992**, *25*, 1284.
(19) Hall, C.; Helfand, E. *J. Chem. Phys.* **1982**, *77*, 3275.
(20) Lindsey, C. P.; Patterson, G. D. *J. Chem. Phys.* **1980**, *73*, 3348.
(21) Moe, N. E.; Ediger, M. D. *Macromolecules* **1995**, *28*, 2329.
(22) The exact value of τ_0 is unimportant as long as it remains small compared to the inverse of the Larmor frequency. Allowing τ_0 to be a weak function of temperature would not change the fit quality.
(23) Zhu, W.; Gisser, D. J.; Ediger, M. D. *J. Polym. Sci., Polym. Phys. Ed.* **1994**, *32*, 2251. Some small component of a C−H vector's initial orientation remains unrelaxed until the entire chain has had time to reorient.
(24) Santangelo et al. (Santangelo, P. G.; Ngai, K. L.; Roland, C. M. *Macromolecules* **1996**, *29*, 3651) report more recent dynamic mechanical experiments on aPP taken near T_g. The temperature ranges of the two experiments do not quite overlap. Extrapolation of the Santangelo's data to higher temperature does not match the data in ref 13. No comment is made on the apparent discrepancy. This discrepancy may due to the widening of the distribution of relaxation times as T_g is approached.
(25) Ediger, M. D. *J. Non-Cryst. Solids* **1998**, 235.
(26) The difference between C−C and C−H vector orientation autocorrelation functions is minimal. Private communication from Doros Theodorou.
(27) A source of ambiguity in making this comparison is that the correlation functions in ref 7 do not decay to zero over the length of the trajectory, requiring extrapolation to longer times. Antoniadis et al. used the KWW function, which lacks the fast exponential of the modified KWW distribution (eq 11) used to fit the NMR data. We found that using the modified KWW function instead to extrapolate the simulation data leads to some improvement in the overall comparisons in Figures 8 and 10.
(28) Qiu, X.; Ediger, M. D. *Macromolecules* **2000**, *33*, 490.

MA991844+